

Carbamoylcholine homologs: synthesis and pharmacology at nicotinic acetylcholine receptors

Anders A. Jensen^{*}, Ivan Mikkelsen¹, Bente Frølund, Karla Frydenvang, Lotte Brehm, Jerzy W. Jaroszewski, Hans Bräuner-Osborne, Erik Falch, Povl Krogsgaard-Larsen

Department of Medicinal Chemistry, The Danish University of Pharmaceutical Sciences, Universitetsparken 2, DK-2100 Copenhagen, Denmark

Received 1 April 2004; received in revised form 17 June 2004; accepted 22 June 2004

Available online 28 July 2004

Abstract

In a recent study, racemic 3-(*N,N*-dimethylamino)butyl-*N,N*-dimethylcarbamate (**1**) was shown to be a potent agonist at neuronal nicotinic acetylcholine receptors with a high selectivity for nicotinic over muscarinic acetylcholine receptors [Mol. Pharmacol. 64 (2003) 865–875]. Here we present the synthesis and pharmacological characterization of a series of analogs of **1**, where the methyl group at C-3 has been replaced by different alkyl substituents. Ring systems have been incorporated into the carbon backbone of some of the molecules, or the amino group has been built into ring systems. Furthermore, the (+)- and (–)-enantiomers of **1** have been separated, and X-ray crystallography has revealed that (–)-**1** possesses (*S*)-configuration. The compounds have been characterized pharmacologically at recombinant nicotinic receptor subtypes. The structure–activity relationship study has provided valuable insight into the mode of interactions of **1** and its analogs with neuronal nicotinic acetylcholine receptors.

© 2004 Elsevier B.V. All rights reserved.

Keywords: Nicotinic acetylcholine receptor; Acetylcholine; Agonist; Carbamoylcholine homolog; Muscarinic

1. Introduction

The neurotransmitter acetylcholine exerts its effects in the central and peripheral nervous systems through two distinct families of receptors: the muscarinic acetylcholine receptors and the nicotinic acetylcholine receptors. The five cloned muscarinic subtypes m1–m5 belong to the G-protein-coupled receptor superfamily (Eglen et al., 2001), whereas the nicotinic acetylcholine receptors belong to a family of pentameric ligand-gated ion channels, which also includes receptors for serotonin, γ -aminobutyric acid and glycine (Corringer et al., 2000; Karlin, 2002). The nicotinic receptors are involved in a wide range of physiological and pathological processes, and the receptors have been proposed as potential therapeutic targets for a number of neurodegener-

ative and psychiatric disorders (Arneric and Brioni, 1999; Gotti et al., 1997; Levin, 2002; Lindstrom, 1997; Paterson and Nordberg, 2000). Furthermore, nicotine replacement therapy is the predominantly used treatment for smoking cessation (Arneric and Brioni, 1999; Levin, 2002).

The nicotinic acetylcholine receptors have traditionally been divided into muscle-type receptors composed of $\alpha 1$, $\beta 1$, γ , ϵ and δ subunits and neuronal receptors made up of $\alpha 2$ – $\alpha 10$ and $\beta 2$ – $\beta 4$ subunits. The neuronal receptors exist either as homomers composed of $\alpha 7$ or $\alpha 9$ subunits or as heteromers made up by various combinations of $\alpha 2$ – $\alpha 6$ with $\beta 2$ – $\beta 4$ subunits or by $\alpha 9$ and $\alpha 10$ subunits (Corringer et al., 2000). The most abundant neuronal nicotinic receptor subtypes in the central nervous system are the $\alpha 4\beta 2$ heteromer and the $\alpha 7$ homomer, whereas the $\alpha 3\beta 4^*$ subtypes ($\alpha 3\beta 4$, $\alpha 3\beta 2\beta 4$, $\alpha 3\alpha 5\beta 4$ and $\alpha 3\alpha 5\beta 2\beta 4$) are the predominant subtypes at ganglionic synapses (Corringer et al., 2000; Gotti et al., 1997; Levin, 2002). In the heteromeric nicotinic receptor, which predominantly is composed of two α and three β subunits, acetylcholine binding takes place at two α/β

^{*} Corresponding author. Tel.: +45 3530 6491; fax: +45 3530 6040.

E-mail address: aaj@dfuni.dk (A.A. Jensen).

¹ Present address: BioImage, Mørkhøj Bygade 28, DK-2860 Søborg, Denmark.

interfaces, whereas the agonist binds to the homomeric receptor at all five subunit interfaces (Brejc et al., 2001; Corringer et al., 2000; Karlin, 2002). In addition to these orthosteric binding sites, nicotinic receptors are subjected to modulation by a wide range of structurally diverse substances of natural origin acting through allosteric sites (Romanelli and Gualtieri, 2003; Tulp and Bohlin, 2002).

The medicinal chemistry efforts in the nicotinic acetylcholine receptor field targeting the orthosteric binding sites have been based extensively on re-design of substances of natural origin such as nicotine, epibatidine, and cytosine (Armeric and Brioni, 1999; Dwoskin and Crooks, 2001; Holladay et al., 1997; Romanelli and Gualtieri, 2003). Although acetylcholine has not attracted similar attention as a lead for nicotinic ligands, important pharmacological tools like carbamoylcholine (or carbachol), *N*-methylcarbamoylcholine (MCC) and *N,N*-dimethylcarbamoylcholine (DMCC) are carbamate analogs of acetylcholine. Carbachol is equipotent at muscarinic receptors and neuronal nicotinic receptor subtypes but the ligand has predominantly been used in the muscarinic receptor field (Eglen et al., 2001). In contrast, MCC and DMCC display pronounced selectivities towards nicotinic over muscarinic receptors, and [^3H]MCC has become a standard nicotinic receptor radioligand (Aboud and Grassi, 1986; Anderson and Armeric, 1994;

Punzi et al., 1991). In a recent study, we presented a series of one-carbon homologs of 2-(*N,N*-dimethylamino)ethyl-*N,N*-dimethylcarbamate (DMCAE), the tertiary amine corresponding to DMCC (Fig. 1) (Jensen et al., 2003). A number of these compounds, including racemic 3-(*N,N*-dimethylamino)butyl-*N,N*-dimethylcarbamate (**1**) and racemic 3-(*N,N*-dimethylamino)butyl-*N*-methylcarbamate (**2**) (Fig. 1), displayed high binding affinities to neuronal nicotinic receptors and pronounced selectivities for nicotinic over muscarinic receptors. Furthermore, the compounds were shown to be agonists at the $\alpha 3\beta 4$ nicotinic acetylcholine receptor subtype. In the present study, we have continued to explore the structure–activity relationships (SARs) for these ligands through the synthesis and pharmacological characterization of a series of analogs of **1**.

2. Materials and methods

2.1. Materials

Culture media, serum, antibiotics, buffers for cell culture, G418 sulfate and blasticidin S HCl were obtained from Invitrogen (Groningen, The Netherlands). [^3H]-(\pm)-epibatidine (for the sake of brevity, named [^3H]epibatidine) and

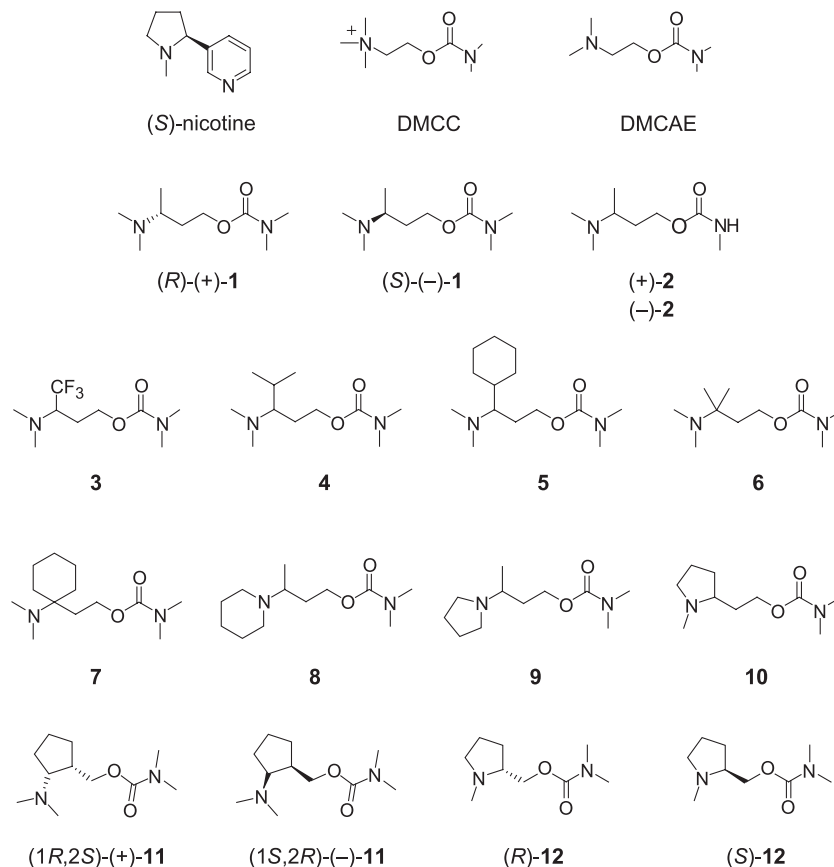


Fig. 1. Chemical structures of (*S*)-nicotine, DMCC, DMCAE and the compounds characterized at nicotinic and muscarinic acetylcholine receptors in this study. The compounds **3–5** and **8–10** are racemic mixtures. Although (*S*)-nicotine, DMCAE, and compounds **1**, **2** and **4–12** are almost completely, but reversibly, protonated at physiological pH, they are depicted in their deprotonated form. Compound **3** is essentially deprotonated at physiological pH.

[³H]N-methylscopolamine were purchased from NEN (Zaventem, Belgium), and [³H]methyllycaconitine was obtained from Tocris (Bristol, UK). Acetylcholine and (S)-nicotine tartrate were obtained from Sigma-RBI (St. Louis, MO) and (±)-epibatidine from Tocris. GF/B and GF/C filters were obtained from Whatman Paper (Gaithersburg, MD). The cDNAs encoding the rat $\alpha 2$, $\alpha 4$, $\alpha 7$ and $\beta 4$ nicotinic acetylcholine receptor subunits were gifts from Dr. James W. Patrick (Baylor College of Medicine, Houston, TX), and the cDNA for the murine 5-HT_{3A} receptor was a gift from Dr. David J. Julius (University of California, San Francisco, CA). Human embryonic kidney (HEK) 293 cell lines stably expressing the rat $\alpha 3\beta 4$ and $\alpha 4\beta 2$ nicotinic receptor subtypes were gifts from Drs. Ken Kellar and Yingxian Xiao (Georgetown University School of Medicine, Washington, DC) and Dr. Joe Henry Steinbach (Washington University School of Medicine, St. Louis, MO), respectively (Sabey et al., 1999; Xiao et al., 1998). The tsA cells were gifts from by Dr. Penelope S.V. Jones (University of California, San Diego, CA). The creation of tsA cell lines stably expressing the $\alpha 2\beta 4$ and $\alpha 4\beta 4$ nicotinic receptor subtypes and the construction of the $\alpha 7/5$ -HT₃ chimera have been described previously (Jensen et al., 2003).

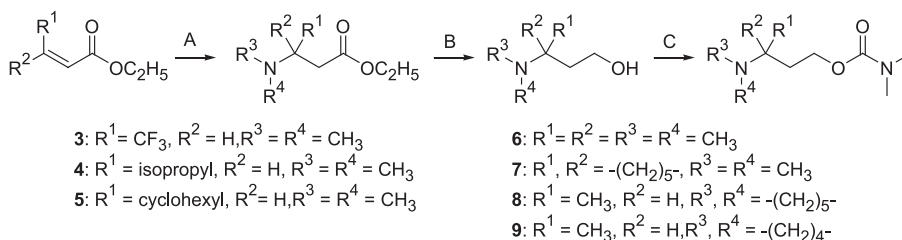
2.2. Chemistry

Compound **1** was optically resolved into the pure enantiomers by salt formation with *O,O'*-dibenzoyltartaric

acid. ¹H NMR analysis (400 MHz) was performed following salt formation with (*R*)-(-)-*O*-acetylmandelic acid, and based on chemical shifts for the *N*-methyl groups, stereochemical purities >95% were observed for each of the enantiomers of **1**. The target compounds **3–9** were all synthesized using the same approach via the appropriate amino alcohols. The amino alcohols were achieved by conjugated addition of a dialkylated amine to the appropriate α,β -unsaturated esters followed by reduction using either lithium aluminium hydride in dry diethyl ether (Scheme 1 in Fig. 2). The α,β -unsaturated esters necessary for these reactions were either commercially available or prepared according to methods described in the literature. The synthesis of the (+)- and (-)-enantiomers of compound **2** was based on (*R*)- and (*S*)-3-aminobutanol, respectively (Kinas et al., 1977). The amino groups of the respective alcohols were dimethylated, and the carbamoyl group was introduced using sodium hydride followed by addition of *N*-methylcarbamoyl chloride.

A mixture of the *cis*-enantiomers of compound **11** was obtained by reductive amination using dimethylamine and catalytic hydrogenation followed by reduction of the resulting amino ester (Scheme 2 in Fig. 2). The two pure *cis*-enantiomers were obtained by diastereomeric salt formation using (*S,S*)-tartaric acid in isopropanol. Most of the tertiary amines, **3–11**, were isolated as fumarate salts from isopropanol. The synthesis of the (*R*)- and (*S*)-enantiomers of

Scheme 1



Scheme 2

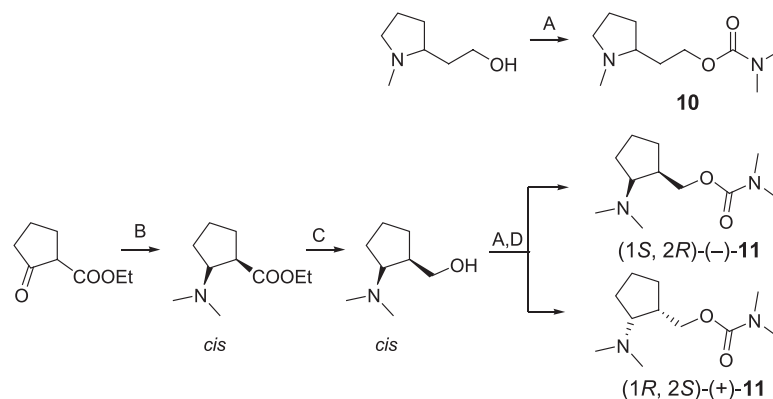


Fig. 2. Synthesis of the target compounds **3–11**. The general structures refer to the compounds presented in Fig. 1. Scheme 1: Synthesis of **3–9**. Reagents: (A) NHR^3R^4 ; (B) LiAlH_4 ; (C) NaH , then *N,N*-dimethylcarbamoyl chloride. Scheme 2: Synthesis of **10** and **11**. Reagents: (A) NaH , then *N,N*-dimethylcarbamoyl chloride; (B) $\text{NH}(\text{CH}_3)_2$, H_2/PtO_2 ; (C) LiAlH_4 ; (D) (*S,S*)-tartaric acid, isopropanol.

compound **12** has been described previously (Søkilde et al., 1996).

All compounds were characterised by ^1H NMR spectroscopy. NMR spectra were recorded on a Bruker AC-200 F spectrometer in CDCl_3 solutions using TMS as an internal standard, or on a Bruker Avance 400 spectrometer equipped with a 5-mm dual probe for $^{13}\text{C}\{^1\text{H}\}$ detection as described in Section 2.3. Melting points were determined in capillary tubes. Analytical thin-layer chromatography (TLC) was carried out using Merck silica gel 60 F254 plates. Elemental analyses were carried out and the results were within $\pm 0.4\%$ of the theoretical values. Optically active compounds were characterized by optical rotation measurements and enantiomeric purity was determined by ^1H NMR spectroscopy of diastereomeric salts.

Experimental details are available by enquiry to the author of correspondence.

2.3. ^{13}C NMR titration experiments

A solution of racemic **1** (30 mg, fumarate salt), **3** (15 mg, hydrochloride salt) and internal standard (sodium 4,4-dimethyl-4-silapentanesulfonate, 5 mg) in $\text{H}_2\text{O}/\text{D}_2\text{O}$ 9:1 (0.6 ml) were adjusted to appropriate pH values with 0.1 or 1.0 M aqueous HCl or 0.1 or 1.0 M aqueous NaOH using a glass microelectrode (MI-412 combination pH electrode, Microelectrodes, Bedford, MA, USA). ^{13}C NMR spectra (100 MHz) were recorded at 27 °C, collecting 64,000 complex data points over a spectral range of 24 kHz. Typically, between 2000 and 8000 transients were collected and Fourier-transformed using Lorentzian line broadening of 1 Hz. The data were collected at 23 different pH values between pH 0.99 and 12.51. Spectral assignments were confirmed by occasional recording of DEPT135 spectra obtained under similar conditions of data acquisition. The ^{13}C chemical shift data were fitted to the equation $\delta_i = (\delta_i^0 \cdot 10^{-\text{pK}_a} + \delta_i^1 \cdot 10^{-\text{pH}}) / (10^{-\text{pK}_a} + 10^{-\text{pH}})$, where δ_i is the observed chemical shifts of the i th carbon atom at a given pH, and δ_i^0 and δ_i^1 are the chemical shift of the i th carbon atom in non-protonated and a fully protonated amine, respectively. Non-linear regression analysis (GraFit v. 4.06, Erithacus Software, Staines, UK) with simultaneous iteration on all carbons of the molecule except for the *N*-methyl groups of the amine moiety (which exhibited exchange broadening due to slow rotation of the amide bond) yielded $\text{pK}_a = 9.85 \pm 0.01$ for **1** and $\text{pK}_a = 4.49 \pm 0.01$ for **3**.

2.4. X-ray crystallography

2.4.1. Crystallographic analysis of the hydrogen (2*S*,3*S*)-*O*,*O'*-dibenzoyltartrate salt of (S)-(-)-**1**

2.4.1.1. Crystal data. Single crystals suitable for X-ray diffraction studies were grown from a solution in 2-propanol by slow evaporation. $\text{C}_{27}\text{H}_{34}\text{N}_2\text{O}_{10}$, M_r 546.6, monoclinic, space group $P2_1$ (No. 4), $a = 7.5891(7)$, $b = 29.796(4)$,

$c = 12.601(1)$ Å, $\beta = 106.706(9)^\circ$, $V = 2729.2(4)$ Å³, $Z = 4$, $D_c = 1.336$ Mg/m³, $F(000) = 1160$, $\mu(\text{MoK}\alpha) = 0.10$ mm⁻¹, crystal size: $0.08 \times 0.12 \times 0.45$ mm.

2.4.1.2. Data collection and reduction. A single crystal was mounted and immersed in a stream of nitrogen [$T = 122(1)$ K]. Data were collected using graphite monochromated MoK α radiation source ($\lambda = 0.71073$ Å) on a KappaCCD diffractometer. Data collection and cell refinement were performed using COLLECT (Nonius, 1999) and DIRAX (Duisenberg, 1992). Data reduction was performed using EvalCCD (Duisenberg, 1998). Correction for absorption was performed using SADABS (Sheldrick, 1996).

2.4.1.3. Structure solution and refinement. Positions of all non-hydrogen atoms were found by direct methods (SHELXS97) (Sheldrick, 1990, 1997b). Full-matrix least-squares refinements (SHELXL97) (Sheldrick, 1997a) were performed on F^2 , minimizing $\sum w(F_o^2 - kF_c^2)^2$, with anisotropic displacement parameters of the non-hydrogen atoms. The position of most of the hydrogen atoms, except for the hydrogen atoms of methyl groups and aromatic rings, were located in subsequent difference electron density maps and refined with fixed isotropic displacement parameters ($U_{\text{iso}} = 1.2U_{\text{eq}}$ for CH and CH₂). The positions of the hydrogen atoms of methyl groups and aromatic rings were included in idealized positions and refined with a riding model with fixed isotropic displacement parameter ($U_{\text{iso}} = 1.2U_{\text{eq}}$ for CH and $1.5U_{\text{eq}}$ for CH₃) of the parent atom. Extinction correction was applied (Sheldrick, 1997a), extinction coefficient: 0.0127(13). Refinement (769 parameters, 9573 unique reflections) converged at $R_f = 0.061$, $wR_F^2 = 0.172$ [8536 reflections with $F_o > 4\sigma(F_o)$]; $w^{-1} = (\sigma^2(F_o^2) + (0.0803P)^2 + 4.9727P)$, where $P = (F_o^2 + 2F_c^2)/3$; $S = 1.117$. The residual electron density varied between -0.31 and 0.69 e Å⁻³. Complex scattering factors for neutral atoms were taken from International Tables for Crystallography as incorporated in SHELXL97 (Sheldrick, 1997a; Wilson, 1995).

The establishment of the absolute configuration of the cation was based on the known chirality of the (2*S*,3*S*)-*O*,*O'*-dibenzoyltartrate ion.

2.4.2. Crystallographic analysis of the hydrogen (2*S*,3*S*)-tartrate salt of (1*R*,2*S*)-(+)-**11**

2.4.2.1. Crystal data. Single crystals suitable for X-ray diffraction studies were grown by vapour diffusion of ether into a solution of the compound in 2-propanol. $\text{C}_{15}\text{H}_{28}\text{N}_2\text{O}_8$, M_r 364.39, orthorhombic, space group $P22_12_1$ (No. 18), $a = 7.525(2)$, $b = 8.4945(13)$, $c = 29.761(5)$ Å, $V = 1902.4(7)$ Å³, $Z = 4$, $D_c = 1.272$ Mg/m³, $F(000) = 784$, $\mu(\text{CuK}\alpha) = 0.87$ mm⁻¹, crystal size: $0.10 \times 0.14 \times 0.50$ mm.

2.4.2.2. Data collection and reduction. A single crystal was mounted and immersed in a stream of nitrogen [$T = 122.0(5)$

K]. Diffraction data were collected on an Enraf-Nonius CAD-4 diffractometer (Enraf-Nonius, 1989), using graphite monochromated CuK α radiation source ($\lambda=1.5418 \text{ \AA}$). Unit cell dimensions were determined by least-squares refinement of 24 reflections (θ range 39–40°). The intensities of the reflections [$3<\theta<75^\circ$, $hk\pm l$ and $-h-k\pm l$; $3<\theta<75^\circ$, $h-k\pm l$ (partly)] were measured in the ω -2 θ scan mode. Three standard reflections monitored every 10^4 s displayed clearly two time segments and a systematic decrease in intensities less than 6% within each segment. Appropriate scaling was performed using the program SCALE3 (Blessing, 1987, 1989). Data were reduced using the programs of Blessing (DREADD) (Blessing, 1987, 1989). Absorption corrections were applied using the program ABSORB (DeTitta, 1985) ($T_{\min}=0.760$, $T_{\max}=0.926$). The equivalent reflections were averaged according to the point group symmetry 222, resulting in 3924 unique reflections ($R_{\text{int}}=0.025$).

2.4.2.3. Structure solution and refinement. The positions of all non-hydrogen atoms were found by direct methods (SHELXS-86) (Sheldrick, 1986). Full-matrix least-squares refinements (SHELXL97) (Sheldrick, 1997a) were performed on F^2 , minimizing $\sum w(F_o^2 - kF_c^2)^2$, with anisotropic displacement parameters of the non-hydrogen atoms. The positions of all hydrogen atoms, except for one methyl group (C11), were clearly located in subsequent difference electron density maps. Hydrogen atoms of the methyl group C11 were included in idealized positions and refined with a riding model with U_{iso} set to $1.5U_{\text{eq}}$ of the parent atom. The positions of the remaining hydrogen atoms were refined freely with U_{iso} set to $1.2U_{\text{eq}}$ (CH, CH₂, and NH) or $1.5U_{\text{eq}}$ (CH₃ and OH) of the parent atom. Extinction correction was applied (Sheldrick, 1997a), extinction coefficient: 0.0028(3). Refinement (304 parameters, 3923 reflections) converged at $R_f=0.028$, $wR_f^2=0.072$ [3692 reflections with $F_o > 4\sigma(F_o)$; $w^{-1}=(\sigma^2(F_o^2)+(0.0453P)^2+0.0520P)$, where $P=(F_o^2+2F_c^2)/3$; $S=1.057$]. The residual electron density varied between -0.16 and 0.19 e \AA^{-3} . Complex scattering factors for neutral atoms were taken from International Tables for Crystallography as incorporated in SHELXL97 (Sheldrick, 1997a; Wilson, 1995). The absolute stereochemistry of the cation was assigned by reference to the known chirality of the hydrogen (2*S*,3*S*)-tartrate ion.

Fractional atomic coordinates, list of anisotropic displacement parameters and a complete list of geometrical data have been deposited in Cambridge Crystallographic Data Centre (Nos. CCDC 233588 and CCDC 233589).

2.5. Cell culture

All cell lines were maintained at 37 °C in a humidified 5% CO₂ incubator in Dulbecco's modified Eagle's medium supplemented with penicillin (100 U/ml), streptomycin (100 µg/ml) and 10% dialyzed fetal calf serum. HEK293 cells stably expressing $\alpha 4\beta 2$ and $\alpha 3\beta 4$ nicotinic receptor

subtypes were cultured in medium containing G418 (0.5 and 0.7 mg/ml, respectively). The tsA cells stably expressing $\alpha 2\beta 4$ and $\alpha 4\beta 4$ nicotinic receptor subtypes were cultured in medium supplemented with G418 (1 mg/ml) and blasticidin (1 µg/ml).

2.6. [³H]Epibatidine binding

For the [³H]epibatidine binding experiments, the stable cell lines were harvested at 80–90% confluency and scraped into assay buffer [140 mM NaCl/1.5 mM KCl/2 mM CaCl₂/1 mM MgSO₄/25 mM HEPES (pH 7.4)], homogenized with a Polytron for 10 s and centrifuged for 20 min at 50,000×*g*. Cell pellets were resuspended in fresh assay buffer, homogenized and centrifuged at 50,000×*g* for another 20 min. Cells were resuspended in assay buffer, and protein concentrations were measured using Bradford Protein Assay with bovine serum albumin as standard (Biorad, Hercules, CA). The total amount of protein in each reaction was 3–5 µg for the $\alpha 4\beta 2$, $\alpha 2\beta 4$ and $\alpha 4\beta 4$ cell lines, whereas amounts below 1 µg were used for $\alpha 3\beta 4$ -HEK293.

Cell membranes were incubated with [³H]epibatidine at concentrations of 10 pM ($\alpha 4\beta 2$), 50 pM ($\alpha 2\beta 4$ and $\alpha 4\beta 4$), or 100 pM ($\alpha 3\beta 4$) in the presence of various concentrations of compounds in a total assay volume of 1 ml. Nonspecific binding was determined in assays with 5 mM (*S*)-nicotine. The total reaction volume was 1 ml, and the assay mixtures were incubated for 4 h at room temperature while shaking. Whatman GF/B filters were presoaked for 1 h in a 0.2% polyethylenimine solution, and binding was terminated by filtration through these filters using a 48-well cell harvester and washing with 4×4 ml ice-cold isotonic NaCl solution. Following this, the filters were dried, 3 ml Opti-Fluor™ (PerkinElmer, Boston, MA) was added, and the amount of bound radioactivity was determined in a scintillation counter. The binding experiments were performed in duplicate at least three times for each compound.

2.7. [³H]Methyllycaconitine binding

For the [³H]methyllycaconitine binding experiments, 2×10^6 cells were split into a 15-cm tissue culture plate a day prior to transfection and transfected with 10 µg $\alpha 7/5$ -HT₃-pCDNA3 using Polyfect as a DNA carrier according to the protocol by the manufacturer (Qiagen, Hilden, Germany). The day after the transfection the medium was changed, and the following day, [³H]methyllycaconitine binding was performed. The cells were scraped into homogenization buffer, homogenized for 10 s in 30 ml homogenization buffer [50 mM Tris-HCl (pH 7.2)] using a polytron, and centrifuged for 20 min at 50,000×*g*. The resulting pellet were homogenized in 30 ml homogenization buffer and centrifuged again. This step was performed twice. The pellets were resuspended in phosphate-buffered saline, and protein concentrations were determined as described above. The protocol used for the binding assay was slightly

modified from that of a previous study (Davies et al., 1999). Five to fifteen microgram protein of $\alpha 7/5$ -HT₃ transfected tsA cells was incubated with 0.5 nM [³H]methyllycaconitine and various concentrations of the test compounds in a total assay volume of 2 ml. Nonspecific binding was determined in reactions with 5 mM (*S*)-nicotine.

The assay mixtures were incubated for 2.5 h at room temperature while shaking. GF/B filters were presoaked for 1 h in a 0.2% polyethylenimine solution, and binding was terminated by filtration through these filters using a 48-well cell harvester and washing with 4×4 ml ice-cold isotonic NaCl solution. Following this, the filters were dried, 3 ml of Opti-Fluor™ was added, and the amount of bound radioactivity was determined in a scintillation counter. The binding experiments were performed in duplicate at least three times for each compound.

2.8. [³H]*N*-methylscopolamine binding

Brain synaptic membranes from male Sprague–Dawley rats were used for the [³H]*N*-methylscopolamine binding assay, and tissue preparation was performed as previously described (Ransom and Stec, 1988). On the day of the assay, the membrane preparation was quickly thawed, suspended in assay buffer [25 mM sodium phosphate (pH 7.4) supplemented with 5 mM MgCl₂], homogenized and centrifuged at 20,000×*g* at 4 °C for 30 min. This step was repeated once, after which the pellet was resuspended in assay buffer, and protein concentrations were measured as described previously. Membranes (50–100 μg protein) were incubated on ice for 6 h in the presence of 5 pM [³H]*N*-methylscopolamine and 8 different concentrations of the test compounds in a total assay volume of 1 ml. Nonspecific binding was determined in the presence of 10 μM atropine. GF/C filters were presoaked for 1 h in a 0.2% polyethylenimine solution, and binding was terminated by filtration through these filters using a 48-well cell harvester and washing with 3×5 ml ice-cold isotonic NaCl solution. Following this, the filters were dried, 3 ml of Opti-Fluor™ was added, and the amount of bound radioactivity was determined in a scintillation counter. The binding experiments were performed in duplicate at least three times for the compounds tested.

2.9. The FLIPR® Membrane Potential (FMP) assay

The compounds were characterized functionally at the $\alpha 3\beta 4$ -HEK293 cell line (Xiao et al., 1998) using the FLIPR® Membrane Potential (FMP) assay according to the protocol of the manufacturer (Molecular Devices, Crawley, UK). Cells were split into poly-D-lysine-coated 96-well black Opti-plates (BD Biosciences, Bedford, MA) in Dulbecco's modified Eagle's medium supplemented with penicillin (100 U/ml), streptomycin (100 μg/ml), 10% dialyzed fetal calf serum, and 0.7 mg/ml G-418. After 16–24 h, the medium was aspirated, and 50 μl fresh medium

containing 2 μM atropine was added to each well. Then 50 μl of loading buffer (dye dissolved in Hanks Buffered Saline Solution supplemented with 20 mM HEPES, pH 7.4) was added to each well, and the plate was incubated at 37 °C in a humidified 5% CO₂ incubator for 30 min. Thus, the final concentration of atropine in the assay was 1 μM. The plate was assayed in a NOVOstar™ apparatus (BMG Labtechnologies, Offenburg, Germany) measuring emission at 560 nm caused by excitation at 530 nm. Data points were measured at room temperature a total of 77 times at various intervals during a period of 1 min. Three of the recordings were done prior to application of 33 μl agonist solution (agonists were diluted in Hanks Buffered Saline Solution supplemented with 20 mM HEPES, pH 7.4). The experiments were performed in duplicate at least three times for each compound. The concentration–response curve for each of the compounds was constructed based on the maximal responses obtained at the eight different concentrations used.

2.10. Data analysis

Data from the binding experiments were fitted to the equation % Bound = 100% Bound / (1 + ([L]/IC₅₀)^{*n*}), and *K*_i values determined using the equation Cheng–Prusoff *K*_i = IC₅₀ / (1 + [L]/*K*_D), where [L] is the radioligand concentration, *n* the Hill coefficient, and *K*_D the dissociation constant. Since the [³H]epibatidine and [³H]methyllycaconitine concentrations used were lower than the *K*_D values determined for the respective nicotinic receptor subtypes (Baker et al., 2004; Jensen et al., 2003; Parker et al., 1998) and the [³H]*N*-methylscopolamine concentrations used were lower than the *K*_D values determined for all five muscarinic receptor subtypes (Dörje et al., 1991), it was deduced from this equation that the *K*_i values for the compounds were similar to the obtained IC₅₀ values. Data from the functional experiments were fitted to the simple mass equation: *R* = *R*_{basal} + [*R*_{max} / (1 + (EC₅₀/[A])^{*n*})], where [A] is the concentration of agonist, *n* the Hill coefficient, and *R* the response. Curves were generated by nonweighted least-squares fits using the program KaleidaGraph 3.6 (Synergy Software, Reading, PA).

3. Results

3.1. Crystallography

The absolute configurations of the cations of (*S*)-(–)-**1** [(*S*)-(–)-*N,N*-dimethyl-3-(dimethylaminocarbonyloxy)-1-methylpropyl]ammonium] and (1*R*,2*S*)-(+)-**11** [(1*R*,2*S*)-(+)-*N,N*-dimethyl-2-(dimethylaminocarbonyloxymethyl)-cyclopentyl]ammonium] were unequivocally determined by X-ray crystallographic analyses of the hydrogen (2*S*,3*S*)-*O,O'*-dibenzoyltartrate and hydrogen (2*S*,3*S*)-tartrate salts, respectively. Perspective drawings of the ions are shown in Figs. 3 and 4.

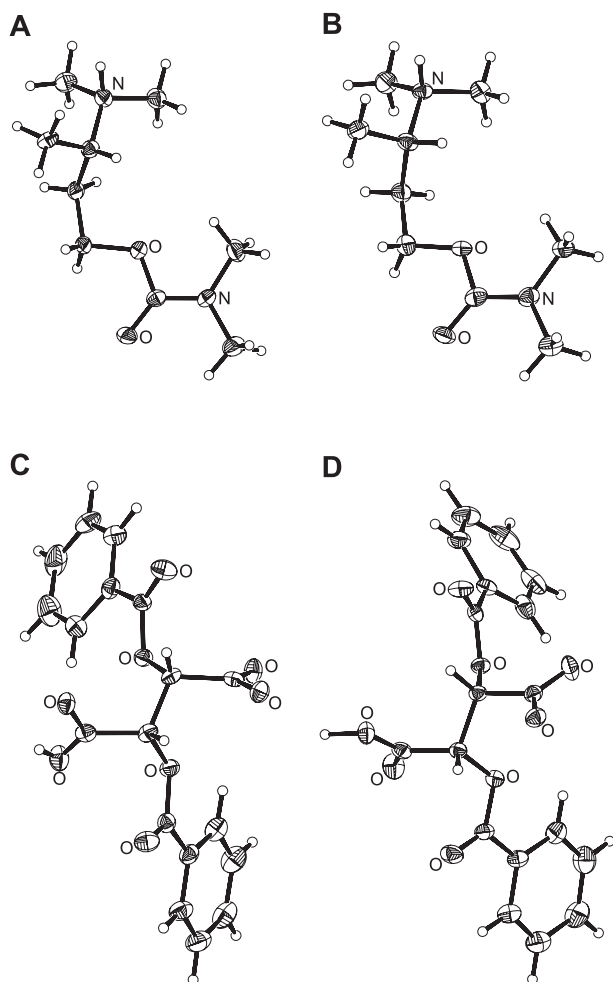


Fig. 3. X-ray structure of (*S*)-(-)-**1**, hydrogen (*2S,3S*)-*O,O'*-dibenzoyltartrate acid. Perspective drawings (ORTEPII) (Johnson, 1976) of the two crystallographically independent cations (A and B) and the two crystallographically independent anions (C and D) found in the asymmetric unit of the crystal structure. The crystal packing reveals differences in the surroundings and intermolecular contacts for the equivalent ions giving rise to small conformationally differences between equivalent ions, the largest being the conformations of the benzoyl moieties of the tartrate ions (C and D). The absolute configuration of the cation is determined to be *S* relative to the known chirality of the hydrogen (*2S,3S*)-*O,O'*-dibenzoyltartrate anion. Displacement ellipsoids of the non-hydrogen atoms are shown at the 50% probability level. Hydrogen atoms are represented by spheres of arbitrary size.

3.2. Competition binding to recombinant nicotinic receptor subtypes

The carbamoylcholine homologs were characterized in competition binding assays to the heteromeric $\alpha 4\beta 2$, $\alpha 2\beta 4$, $\alpha 3\beta 4$ and $\alpha 4\beta 4$ receptors stably expressed in HEK293 or tsA cells and to a $\alpha 7/5$ -HT₃ chimera transiently expressed in tsA cells. In a previous study we have demonstrated that the pharmacological characteristics of the $\alpha 4\beta 2$, $\alpha 2\beta 4$, $\alpha 3\beta 4$ and $\alpha 4\beta 4$ cell lines in a [³H]epibatidine binding assay are in excellent agreement with those reported for the recombinant receptors in other studies (Jensen et al., 2003). Since no significant radioligand binding can be obtained to mamma-

lian cells transiently transfected with the $\alpha 7$ nicotinic acetylcholine receptor, we used the $\alpha 7/5$ -HT₃ chimera to estimate the affinities of the carbamoylcholine homologs for the $\alpha 7$ subtype (Eiselé et al., 1993). We and others have previously demonstrated that the pharmacological characteristics of $\alpha 7/5$ -HT₃ chimeras in [³H]methyllycaconitine binding assays are very similar to those of native $\alpha 7$ nicotinic receptors (Baker et al., 2004; Jensen et al., 2003).

The binding properties of the **1** analogs at the recombinant receptor subtypes are given in Table 1, and the profiles of selected compounds in the series at the $\alpha 4\beta 2$ and $\alpha 3\beta 4$ subtypes are shown in Fig. 5. The Hill slopes for the compounds at the five receptors were around unity, except in those cases where no significant inhibition was observed (data not shown). The binding affinities of the compounds at the heteromeric α/β nicotinic receptors spanned from low nanomolar concentrations displayed by (*R*)-(+)-**1** and (+)-**2** at $\alpha 4\beta 2$ to compounds **3** and **8** which were virtually inactive at all receptors (Table 1). In agreement with the observations for the first series of **1** analogs (Jensen et al., 2003), the present compounds displayed very weak binding to the $\alpha 7/5$ -HT₃ chimera (Table 1). (*S*)-**12** exhibited the highest binding affinities of the compounds at this chimera with *K_i* values comparable to those displayed by standard nicotinic agonists like acetylcholine and (*S*)-nicotine.

3.3. Functional characterization at the $\alpha 3\beta 4$ nicotinic receptor subtype

The **1** analogs were characterized functionally at the $\alpha 3\beta 4$ -HEK293 cell line in the FMP assay. The agonist pharmacology profiles of $\alpha 3\beta 4$ and other nicotinic receptor subtypes in this assay have previously been demonstrated to be similar to data obtained in electrophysiological recordings and other fluorescence-based assays (Fitch et al., 2003; Jensen et al., 2003). Acetylcholine and (*S*)-nicotine were used as reference compounds, and the potencies of the two

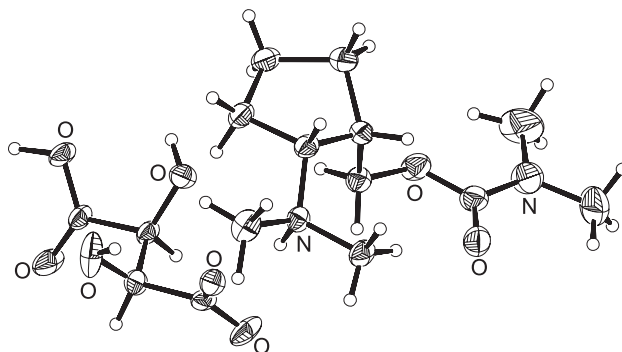


Fig. 4. X-ray structure of (*1R,2S*)-(+)-**11**, hydrogen (*2S,3S*)-tartaric acid. Perspective drawings (ORTEPII) (Johnson, 1976) of the ions. The absolute stereochemistry of the cation has been assigned by reference to the known chirality of the hydrogen (*2S,3S*)-tartrate ion. Displacement ellipsoids of the non-hydrogen atoms are shown at the 50% probability level. Hydrogen atoms are represented by spheres of arbitrary size.

Table 1
Binding characteristics at recombinant nicotinic acetylcholine receptors

Compound	$\alpha 4\beta 2$	$\alpha 2\beta 4$	$\alpha 3\beta 4$	$\alpha 4\beta 4$	$\alpha 7/5\text{-HT}_3$
Acetylcholine ^a	0.033 [7.5±0.11]	0.11 [7.0±0.05]	0.62 [6.2±0.08]	0.058 [7.2±0.12]	170 [3.8±0.08]
(S)-nicotine ^a	0.0083 [8.1±0.12]	0.083 [7.1±0.01]	0.29 [6.5±0.05]	0.074 [7.1±0.11]	31 [4.5±0.07]
1^a	0.017 [7.8±0.04]	0.10 [7.0±0.02]	0.37 [6.4±0.04]	0.066 [7.2±0.09]	>1000 [<3]
2^a	0.013 [7.9±0.21]	0.53 [6.3±0.07]	10 [5.0±0.07]	2.6 [5.6±0.08]	>1000 [<3]
(R)-(+)- 1	0.0062 [8.2±0.07]	0.052 [7.3±0.05]	0.27 [6.6±0.06]	0.062 [7.2±0.13]	>1000 [<3]
(S)-(-)- 1	0.11 [7.0±0.12]	0.25 [6.6±0.09]	1.6 [5.8±0.08]	0.26 [6.6±0.10]	>1000 [<3]
(+)- 2	0.0069 [8.2±0.03]	0.39 [6.4±0.04]	9.6 [5.0±0.09]	0.93 [6.0±0.15]	>1000 [<3]
(-)- 2	0.29 [6.5±0.12]	1.5 [5.8±0.06]	5.2 [5.3±0.08]	1.7 [5.8±0.01]	>1000 [<3]
3	>1000 [<3]	>1000 [<3]	>1000 [<3]	>1000 [<3]	>1000 [<3]
4	4.8 [5.3±0.15]	2.8 [5.6±0.15]	9.9 [5.0±0.07]	2.2 [5.7±0.05]	>1000 [<3]
5	95 [4.0±0.15]	41 [4.4±0.09]	49 [4.3±0.06]	19 [4.7±0.11]	370 [3.4±0.13]
6	0.59 [6.2±0.09]	0.85 [6.1 ± 0.13]	6.2 [5.2±0.13]	0.29 [6.5±0.12]	340 [3.4±0.06]
7	19 [4.7±0.09]	8.3 [5.1±0.11]	15 [4.8±0.04]	4.6 [5.3±0.11]	470 [3.3±0.08]
8	470 [3.3±0.11]	>1000 [<3]	>1000 [<3]	>1000 [<3]	>1000 [<3]
9	28 [4.6±0.03]	150 [5.8±0.11]	110 [3.9±0.11]	72 [4.1±0.10]	>1000 [<3]
10	0.67 [6.2±0.05]	0.40 [6.4±0.13]	1.5 [5.8±0.09]	1.5 [5.8±0.10]	>1000 [<3]
(1R,2S)-(+)- 11	0.32 [6.5±0.32]	1.7 [5.8±0.09]	14 [4.8±0.12]	2.0 [5.7±0.03]	290 [3.5±0.13]
(1S,2R)-(-)- 11	0.19 [6.7±0.15]	1.3 [5.9±0.08]	13 [4.9±0.08]	2.6 [5.6±0.05]	320 [3.5±0.11]
(R)- 12	0.16 [6.8±0.04]	0.39 [6.4±0.08]	1.4 [5.8±0.04]	0.48 [6.3±0.02]	104 [4.1±0.08]
(S)- 12	0.16 [6.8±0.09]	0.36 [6.5±0.10]	1.1 [6.0±0.05]	0.19 [6.7±0.08]	51 [4.3±0.12]

The K_i values of the respective compounds in competition binding experiments are given in μM with $pK_i \pm \text{S.E.M.}$ values in brackets. The $\alpha 4\beta 2$ and $\alpha 3\beta 4$ subtypes were stably expressed in HEK293 cells, the $\alpha 2\beta 4$ and $\alpha 4\beta 4$ subtypes were stably expressed in tsA cells, and $\alpha 7/5\text{-HT}_3$ was transiently expressed in tsA cells. The [³H]epibatidine and [³H]methyllycaconitine binding experiments were performed as described in Materials and methods. All compounds were characterized in duplicate at least three times.

^a Data for acetylcholine, (S)-nicotine and the racemic compounds 1 and 2 are from Jensen et al. (2003).

agonists were in excellent agreement with those obtained in our previous study (Jensen et al., 2003).

The majority of the **1** analogs were agonists at the $\alpha 3\beta 4$ subtype (Fig. 6A; Table 2). However, with the exception of (R)-(+)-**1**, all compounds in the new series displayed significantly reduced potencies as compared to **1**. Furthermore, some of the compounds displayed maximal responses considerably lower than those of **1** and acetylcholine (Table 2). Compounds **3** and **8** were inactive both as agonists and antagonists (using 20 μM acetylcholine as agonist) at concentrations up to 3 mM (Table 2). There was a nice correlation between the potencies and binding affinities displayed by the compounds at the $\alpha 3\beta 4$ subtype ($r^2=0.85$, Fig. 6B).

3.4. Competition binding to native muscarinic receptors

The binding properties of selected compounds from the compound series at native muscarinic receptor sites were determined in a [³H]*N*-methylscopolamine binding assay using rat brain membranes. The K_i values for all the compounds tested were in the mid-micromolar range (Table 3). The majority of the compounds, and (R)-(+)-**1** and (S)-**12** in particular, displayed significant degrees of selectivities for both the $\alpha 4\beta 2$ and the $\alpha 3\beta 4$ nicotinic receptor subtype over muscarinic receptors, whereas compound (+)-**2** displayed a high selectivity for $\alpha 4\beta 2$ but similar binding affinities at the $\alpha 3\beta 4$ nicotinic receptor and native muscarinic receptors (Table 3).

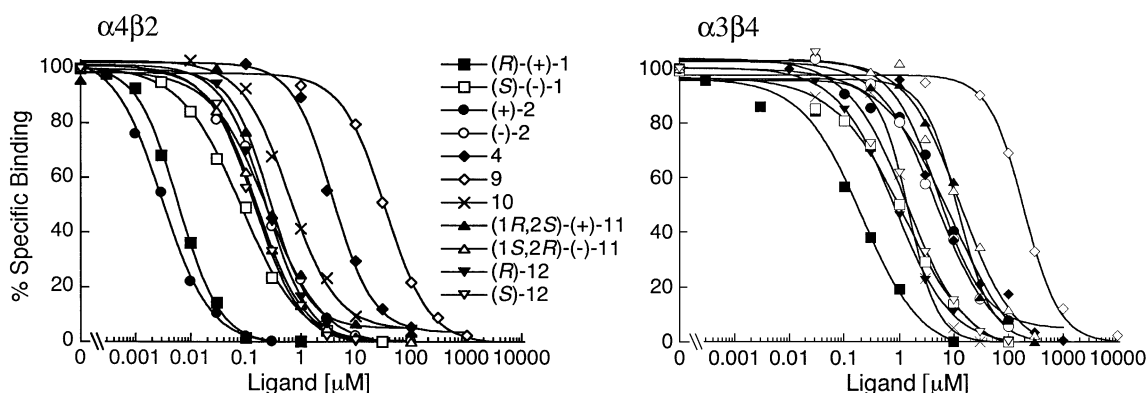


Fig. 5. Binding characteristics of compounds at the $\alpha 4\beta 2$ and $\alpha 3\beta 4$ nicotinic acetylcholine receptor subtypes. Concentration-inhibition curves for (R)-(+)-**1**, (S)-(-)-**1**, (+)-**2**, (-)-**2**, **4**, **9**, **10**, (1R,2S)-(+)-**11**, (1S,2R)-(-)-**11**, (R)-**12** and (S)-**12** at the $\alpha 4\beta 2$ and $\alpha 3\beta 4$ subtypes in the [³H]epibatidine binding assay. Radioligand concentrations of 10 and 100 pM were used for $\alpha 4\beta 2$ and $\alpha 3\beta 4$, respectively. Error bars have been omitted for clarity.

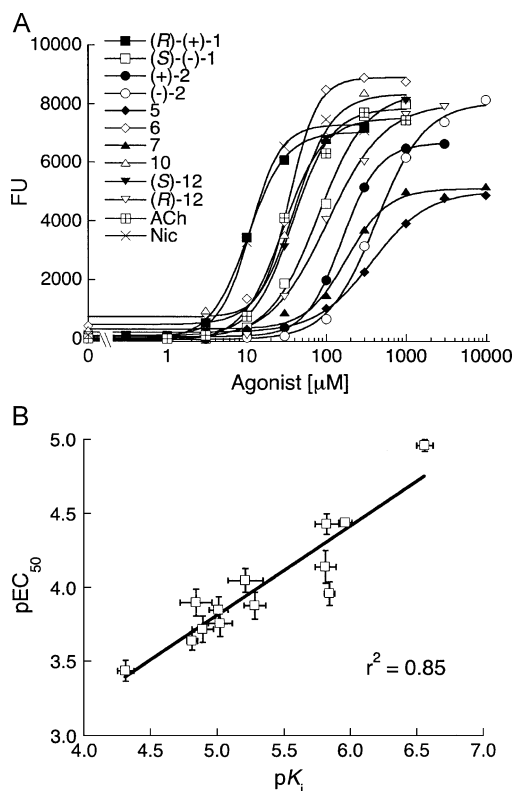


Fig. 6. Functional characteristics of compounds at the $\alpha 3\beta 4$ nicotinic acetylcholine receptor. (A) Concentration-response curves for (R) -(+)-**1**, (S) -(-)-**1**, (+)-**2**, (-)-**2**, **5**, **6**, **7**, **10**, (S) -**12** and (R) -**12** and standard agonists acetylcholine and (S) -nicotine at the $\alpha 3\beta 4$ nicotinic acetylcholine receptor. Error bars have been omitted for clarity. FU, fluorescence unit. (B) Correlation between pK_i and pEC_{50} values of (R) -(+)-**1**, (S) -(-)-**1**, (+)-**2**, (-)-**2**, **4**, **5**, **6**, **7**, **10**, $(1R,2S)$ -(+)-**11**, $(1S,2R)$ -(-)-**11**, (R) -**12** and (S) -**12** at the $\alpha 3\beta 4$ subtype.

3.5. ^{13}C NMR titration experiments

Determination of apparent, thermodynamic acidity constants for **1** and **3** were performed by ^{13}C NMR titration using multiple regression analysis (Jaroszewski et al., 1996; Perrin and Fabian, 1996). In order to minimize errors originating from the pH measurements, the two compounds were titrated as a mixture in a 1:1.8 molar ratio, the individual resonances being easily assigned from line intensities and by comparison with spectra of reference solutions containing one compound only. The obtained pK_a values of **1** and **3**, respectively, 9.85 and 4.49, are in agreement with literature data for related compounds (Bissell and Finger, 1959; Hine et al., 1974). Examples of ^{13}C NMR titration curves are shown in Fig. 7.

4. Discussion

In our recent SAR study of a series of DMCAE homologs including the racemic compounds **1** and **2** we identified the following molecular characteristics as crucial determinants for the activities of the compounds at neuronal nicotinic

Table 2
Functional characteristics of compounds at the $\alpha 3\beta 4$ nicotinic acetylcholine receptor

Compound	EC_{50}	n_H	R_{max}
Acetylcholine	32 [4.5±0.06]	1.6 [1.3–1.8]	100
(S) -nicotine	13 [4.9±0.11]	2.1 [1.8–2.3]	110±7
1 ^a	11 [4.9±0.06]	1.6 [1.4–1.8]	110±9
2 ^a	200 [3.7±0.05]	2.1 [1.8–2.5]	100±12
(R) -(+)- 1	11 [5.0±0.04]	1.7 [1.4–2.0]	94±9
(S) -(-)- 1	72 [4.1±0.11]	1.6 [1.3–1.9]	110±13
(+)- 2	170 [3.8±0.09]	2.1 [1.8–2.5]	93±11
(-)- 2	130 [3.9±0.09]	1.7 [1.4–1.9]	96±8
3 ^b	>3000 [<2.5]	–	–
4	140 [3.9±0.09]	1.3 [1.1–1.5]	78±10
5	360 [3.4±0.07]	1.5 [1.3–1.8]	56±13
6	90 [4.1±0.08]	2.1 [1.9–2.3]	110±8
7	230 [3.6±0.06]	1.3 [1.1–1.6]	48±14
8 ^b	>3000 [<2.5]	–	–
9 ^c	>3000 [<2.5]	–	–
10	37 [4.4±0.07]	2.1 [1.7–2.5]	96±15
$(1R,2S)$ -(+)- 11	130 [3.9±0.09]	2.3 [2.2–2.5]	89±8
$(1S,2R)$ -(-)- 11	190 [3.7±0.09]	1.4 [1.1–1.8]	100±10
(R) - 12	110 [4.0±0.08]	1.9 [1.5–2.3]	110±8
(S) - 12	36 [4.4±0.01]	1.6 [1.5–1.7]	93±13

n.d., not determined.

The EC_{50} and n_H values obtained for the compounds at the $\alpha 3\beta 4$ -HEK293 cell line in the FLIPR Membrane Potential assay. The experiments were performed as described in Materials and methods. Each experiment was performed in duplicate at least three times. EC_{50} values are given in μM with confidence intervals in brackets, and R_{max} values for the compounds are given as % of R_1 mM acetylcholine±S.E.M.

^a Data for the racemic compounds **1** and **2** are from Jensen et al. (2003).

^b Inactive both as agonist and antagonist (against 20 μM ACh).

^c Weak agonist response at 3 mM.

acetylcholine receptors: (1) the tertiary nature of the amino group; (2) the carbon backbone between the amino group and the carbamate group (three separating carbon atoms being optimal); (3) the C-1, C-2 and C-3 carbon substituents

Table 3

Binding characteristics of selected compounds to native muscarinic acetylcholine receptors

Compound	K_i [pK_i ±S.E.M.]	n_H	$K_i/K_i^{\alpha 4\beta 2}$	$K_i/K_i^{\alpha 3\beta 4}$
1 ^a	51 [4.3±0.08]	0.85 [0.81–0.89]	3000	140
2 ^a	74 [4.1±0.02]	0.96 [0.73–1.2]	5700	7.1
(R) -(+)- 1	47 [4.3±0.01]	0.95 [0.74–1.2]	7600	170
(S) -(-)- 1	46 [4.3±0.05]	0.90 [0.85–0.95]	430	29
(+)- 2	20 [4.7±0.08]	0.91 [0.78–1.1]	2900	2.1
(-)- 2	70 [4.2±0.01]	0.82 [0.78–0.86]	240	13
$(1R,2S)$ -(+)- 11	57 [4.2±0.01]	0.87 [0.86–0.89]	180	3.9
$(1S,2R)$ -(-)- 11	101 [4.0±0.05]	1.03 [0.93–1.1]	520	8.4
(R) - 12	31 [4.5±0.01]	0.84 [0.76–0.96]	201	22
(S) - 12	130 [3.9±0.06]	0.92 [0.81–1.0]	780	110

The [3H]N-methylscopolamine competition binding assay to rat brain membranes was performed as described in Materials and methods. K_i values are given in μM with pK_i ±S.E.M. values in brackets, and n_H values are given with confidence intervals in brackets. The ratios between the K_i values at the native muscarinic receptors and the K_i values at the $\alpha 4\beta 2$ and $\alpha 3\beta 4$ nicotinic receptor subtypes are given as well.

^a Data for the racemic compounds **1** and **2** are from Jensen et al. (2003).

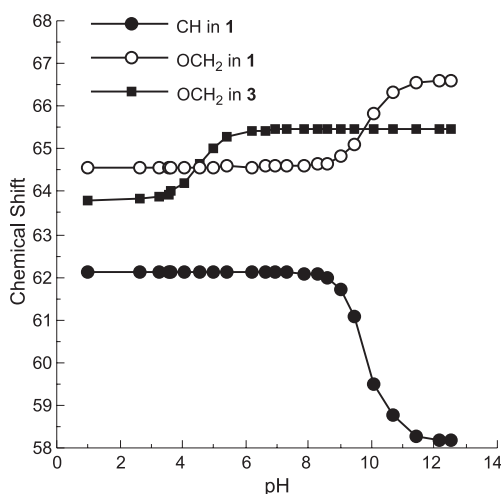


Fig. 7. Selected ^{13}C NMR titration curves obtained for a mixture of **1** and **3** (100 MHz, 27 °C, $\text{H}_2\text{O}/\text{D}_2\text{O}$ 9:1).

(a C-3 methyl group increased the nicotinic activity significantly, whereas methyl groups at C-1 and C-2 diminished nicotinic receptor binding dramatically); and (4) the substituents on the carbamate nitrogen (aryl or alkyl substituents larger than ethyl groups reduced the nicotinic activity significantly) (Jensen et al., 2003). Using compound **1** as a lead we now present a new series of compounds, which further elucidates the SARs for this series.

An X-ray crystal structure analysis of the hydrogen (2*S*,3*S*)-*O*,*O'*-dibenzoyl tartrate salt of the (–)-enantiomer of **1** revealed that it possesses the (*S*)-configuration (Fig. 3). Consequently, it was established that the more active of the two enantiomers of **1** is the (*R*)-(+)-form (Table 1). (*R*)-(+)-**1** and (+)-**2** displayed similar selectivity profiles at the heteromeric nicotinic receptors as those exhibited by the racemic mixtures of the compounds in our recent study (Table 1) (Jensen et al., 2003). For example, the $K_i^{\alpha 3\beta 4}/K_i^{\alpha 4\beta 2}$ ratios for (*R*)-(+)-**1** and (+)-**2** were 43 and 1400, respectively, compared to ratios of 22 and 770 for the racemic **1** and **2**, respectively (Table 1). Hence, (+)-**2** displayed an even higher degree of selectivity for $\alpha 4\beta 2$ over $\alpha 3\beta 4$ in the binding assay than the racemic compound (Jensen et al., 2003). Interestingly, (*R*)-(+)-**1** and (+)-**2** displayed 18- and 42-fold higher binding affinities at the $\alpha 4\beta 2$ subtype than their corresponding (–)-forms, whereas the (–)-enantiomer/(+)-enantiomer ratios at the three $\beta 4$ -containing receptors only were 4–6 and 0.5–4, respectively. Hence, the absolute stereochemistry of the molecules appears to be more important for the $\beta 2$ -containing nicotinic receptor subtypes than for the $\beta 4$ receptors, the (–)-enantiomers displayed unique selectivity profiles as compared to their corresponding (+)-forms. Based on the pharmacological profiles of the enantiomers of **1** and **2**, it is reasonable to assume that the (+)- and (–)-enantiomers of **2** represent the (*R*)- and (*S*)-configurations, respectively, as experimentally established for the **1** enantiomers. However, the (*S*)/(–)- and (*R*)/(+)-relationships for compound **1** cannot be assumed to apply for

all the 3-(*N,N*-dimethylamino)butylcarbamate compounds presented in our previous study (Jensen et al., 2003) or compounds **3–5** and **8–10** in this study (Fig. 1). Interestingly, stereochemistry did not appear to be as important for the enantiomers of compounds **11** and **12**, which displayed similar binding affinities at all the recombinant nicotinic receptors (Table 1).

In our recent study, we reported that the C-3 methyl group of **1** is crucial for its nicotinic activity (Jensen et al., 2003). Whereas replacement of this methyl group with a hydrogen atom had a detrimental effect on binding affinity, introduction of an ethyl group in this position only decreased the binding affinities at the different α/β nicotinic receptor subtypes two- to eightfold (Jensen et al., 2003). In the present study, we therefore probed the spatial surroundings of the C-3 carbon further by introducing other alkyl substituents (compounds **3–7**). Introduction of an isopropyl group (compound **4**) decreased the binding affinity 300- and 30-fold as compared to **1** at $\alpha 4\beta 2$ and the $\beta 4$ -containing subtypes, respectively. This is a quite substantial negative effect on binding affinity compared to that observed for the closely related ethyl analog (Jensen et al., 2003). Introduction of a cyclohexyl ring (compound **5**), a bulkier C-3 substituent, decreased the binding affinities to the heteromeric nicotinic receptor subtypes even further, and bis-methylation of C-3 (compound **6**) reduced binding affinities at $\alpha 4\beta 2$, $\alpha 2\beta 4$, $\alpha 3\beta 4$ and $\alpha 4\beta 4$ with a factor of 35-, 9-, 17- and 4-fold, respectively, as compared to **1** (Table 1). The decreased binding affinity of this compound could either originate from sterical obstruction in the binding pocket to the “additional” C-3 methyl group or by an unfavourable spatial orientation of the two methyl groups in **6** for nicotinic receptor binding as compared to the single methyl group at C-3 in **1**. In light of the reduced binding properties displayed by compounds **4** and **5**, it was not surprising that cyclization of the two C-3 methyl groups in **6** into a cyclohexane group further reduced the nicotinic activity (compound **7**).

The detrimental effect on the nicotinic receptor binding of the introduction of a trifluoromethyl group in the C-3 position was striking (compound **3**). Since the size of the trifluoromethyl group is comparable to that of the corresponding methyl group in **1**, differences in electron distribution had to account for the dramatic differences in the activities of the two compounds. This was confirmed by ^{13}C NMR titration experiments, where the pK_a values for the amino groups in compound **1** and **3** were determined to be 9.85 and 4.49, respectively. Since this means that **1** is completely protonated at pH 7.4, whereas **3** is essentially deprotonated, it is hardly surprising that the two compounds displayed >10,000-fold difference in binding affinities and that compound **3** was inactive at all the nicotinic receptors (Table 1). Hence, the nicotinic activity of the **1** analog is clearly determined not only by the bulk of its C-3 substituent but also by its contribution to the electron density at the basic amino group next to it.

In our recent study, introduction of piperidine or pyrrolidine ring systems in the carbamate group of **1** gave rise to two quite potent compounds (Jensen et al., 2003). In contrast, introduction of piperidine or pyrrolidine rings as the basic amino group of the compounds decreased binding affinities at the four α/β nicotinic receptor subtypes more than 1000-fold (compounds **8** and **9** in Table 1). It is well established that the basic amino group of the nicotinic agonist binds in a receptor pocket formed by five aromatic amino acids due to cation– π interactions (Brejc et al., 2001; Zhong et al., 1998). Thus, there does not appear to be sufficient space in the “aromatic pocket” to accommodate the binding of the quite bulky piperidine or pyrrolidine rings of compounds **8** and **9**.

In the remaining compounds in the series, we introduced ring structures in the 3-(*N,N*-dimethylamino)butyl part of **1** in an attempt to restrict the conformational flexibility of the molecule and hereby achieve more potent and/or subtype-selective compounds. Cyclization of the C-3 methyl group and one of the *N*-methyl groups into a pyrrolidine ring gave rise to compound **10**, which interestingly displayed similar high-nanomolar/low-micromolar K_i values at all four heteromeric nicotinic receptor subtypes (Table 1). (1*R*,2*S*)-(+)- and (1*S*,2*R*)-(–)-**11**, where a cyclopentane ring was introduced between C-2 and C-3, displayed 10- to 40-fold reduced binding affinities at the heteromeric nicotinic receptors as compared to **1**. The relatively high binding affinities of the two *cis*-enantiomers of **11** are remarkable, considering that the introduction of a methyl group at C-2 in the DMCAE homolog has been shown to completely eliminate nicotinic receptor binding (Jensen et al., 2003). Clearly, the five-membered ring in the two *cis*-enantiomers of **11** must be oriented in the binding pocket in a manner different from that of the C-2 methyl group substituent.

In compounds (*R*)- and (*S*)-**12**, the carbon backbone of **10** has been shortened by one methylene group, providing hybrid compounds composed of the pyrrolidine ring of nicotine and the carbamate moiety of DMCAE (or DMCC). There are multiple examples of molecular hybridization in the nicotinic receptor field, some of which have resulted in compounds with affinities and potencies comparable to the parent compounds (Holladay et al., 1997; Romanelli and Gualtieri, 2003). For example, hybridization of epibatidine with compounds like anatoxin-a and ABT-418 have given rise to ligands with very interesting pharmacological profiles (Sharples et al., 2000; Silva et al., 2002). Apart from (*R*)-(+)-**1** and (+)-**2**, compounds (*R*)- and (*S*)-**12** displayed the highest binding affinities in the present series (Table 1). It has been proposed that the protonated cationic center of nicotine binds to the aromatic pocket of the nicotinic receptor different from that of the quaternary amino group of acetylcholine (Beene et al., 2002). Since DMCC is likely to bind to the nicotinic receptor in a similar way as acetylcholine, the different binding modes of the parent compounds nicotine and DMCC could explain the lower binding affinities of the two hybrid compounds. On

the other hand, the nicotine/DMCC hybrids, (*R*)- and (*S*)-**12**, displayed slightly higher affinities at the nicotinic receptors than their one-carbon higher homolog, the nicotine/**1** hybrid, compound **10** (Table 1).

All compounds in this series were determined to be agonists at the $\alpha 3\beta 4$ subtype, except **3** and **8**, which were completely inactive both as agonists and antagonists at the receptor (Table 2). In agreement with the binding data, (*R*)-(+)-**1** and (+)-**2** were found to be equipotent with the racemic mixtures of **1** and **2**, respectively, and in general the EC_{50} values of the compounds correlated well with their binding affinities at the receptor (Fig. 6B). Interestingly, compounds **4**, **5** and **7** were found to be partial agonists at $\alpha 3\beta 4$ (Table 2), whereas the compounds in our previous series all displayed maximal responses similar to that of acetylcholine (Jensen et al., 2003). Hence, in addition to the marked impairments in receptor affinities and potencies the introduction of bulkier C-3 substituents in **1** (Fig. 1) also reduced the efficacy of the agonist at the $\alpha 3\beta 4$ subtype, at least in this functional assay.

In conclusion, the present SAR study provides valuable information for the future design of molecules in this series of carbamoylcholine homologs. It has been established that both enantiomers of **1** and **2** possess nicotinic activity, and the (*R*)-(+)-configuration has been identified as the most potent of the two enantiomers of **1**. Concerning the C-3 substituent of the analogs of **1**, a single methyl group appears to be the optimal for nicotinic receptor binding. However, so far we have only introduced alkyl groups in this position, and it would be interesting to introduce other types of groups in this position of the molecule. Although the incorporation of ring systems into the carbon backbone of **1** did not result in more potent compounds, it did give rise to compounds with interesting subtype-selectivity profiles. The size of the ring systems in compounds **10** and **11** is likely to present steric hindrances to optimal receptor binding, and thus incorporation of smaller ring systems would be a way to proceed in the future. The same applies for the replacement of the amino group of **1** with heterocyclic ring systems, as pyrrolidine and pyridine rings clearly are too bulky to fit into the “aromatic cavity” of the binding site of the nicotinic receptor. All in all, the insight into the structural requirements for binding of **1** and its analogs to the nicotinic receptors obtained in this study will be highly valuable in our continuing work with this series of nicotinic acetylcholine receptor ligands.

Acknowledgements

The authors want to thank the staff of the Department of Medicinal Chemistry at H. Lundbeck, in particular Drs. Haleh Ahmadian, Bitten Hansen and Jens Schjøtt for their contributions to the synthesis of some of the compounds presented in the study. The technical assistance of Flemming Hansen (University of Copenhagen) with collecting X-ray

data is gratefully acknowledged, and Drs. Preben Hansen (University of Copenhagen) and G. Cornali (Leo Pharmaceuticals) are acknowledged for their help with the elemental analyses. Drs. James W. Patrick and David J. Julius are thanked for their kind gifts of nicotinic receptor and 5-HT₃ receptor cDNAs. Drs. Ken Kellar, Yingxian Xiao and Joe Henry Steinbach are thanked for generously providing us with the $\alpha 3\beta 4$ and $\alpha 4\beta 2$ cell lines. This work was supported by the Lundbeck Foundation, the Danish Technical Research Council, the Danish Medical Research Council, the Augustinus Foundation, and the Director Ib Henriksen Foundation.

References

- Abood, L.G., Grassi, S., 1986. [³H]Methylcarbamylcholine, a new radioligand for studying brain nicotinic receptors. *Biochem. Pharmacol.* 35, 4199–4202.
- Anderson, D.J., Arneric, S.P., 1994. Nicotinic receptor binding of [³H]cytisine, [³H]nicotine and [³H]methylcarbamylcholine in rat brain. *Eur. J. Pharmacol.* 253, 261–267.
- Arneric, S.P., Brioni, J.D., 1999. *Neuronal Nicotinic Receptors: Pharmacology and Therapeutic Opportunities*. Wiley-Liss, New York, NY.
- Baker, E.R., Zwart, R., Sher, E., Millar, N.S., 2004. Pharmacological properties of the $\alpha 9\alpha 10$ nicotinic acetylcholine receptors revealed by heterologous expression of subunit chimeras. *Mol. Pharmacol.* 65, 453–460.
- Beene, D.L., Brandt, G.S., Zhong, W., Zacharias, N., Lester, H.A., Dougherty, D.A., 2002. Cation- π interactions in ligand recognition by serotonergic (5-HT_{3A}) and nicotinic acetylcholine receptors: the anomalous binding properties of nicotine. *Biochemistry* 41, 10262–10269.
- Bissell, E.R., Finger, M., 1959. Fluorine-containing nitrogen compounds: I. Trifluoroethylamines. *J. Org. Chem.* 24, 1256–1259.
- Blessing, R.H., 1987. Data reduction and error analysis for accurate single-crystal diffraction intensities. *Crystallogr. Rev.* 1, 3–58.
- Blessing, R.H., 1989. DREADD—data reduction and error analysis for single-crystal diffractometer data. *J. Appl. Crystallogr.* 22, 396–397.
- Brejc, K., van Dijk, W.J., Klaassen, R.V., Schuurmans, M., van Der Oost, J., Smit, A.B., Sixma, T.K., 2001. Crystal structure of an ACh-binding protein reveals the ligand-binding domain of nicotinic receptors. *Nature* 411, 269–276.
- Corringer, P.-J., Le Novère, N., Changeux, J.-P., 2000. Nicotinic receptors at the amino acid level. *Annu. Rev. Pharmacol. Toxicol.* 40, 431–458.
- Davies, A.R.L., Hardick, D.J., Blagbrough, I.S., Potter, B.V.L., Wolstenholme, A.J., Wonnacott, S., 1999. Characterisation of the binding of [³H]methyllycaconitine: a new radioligand for labelling $\alpha 7$ -type neuronal nicotinic acetylcholine receptors. *Neuropharmacology* 38, 679–690.
- DeTitta, G.T., 1985. ABSORB: an absorption correction programme for crystals enclosed in capillaries with trapped mother liquor. *J. Appl. Crystallogr.* 18, 75–79.
- Dörje, F., Wess, J., Lambrecht, G., Tacke, R., Mutschler, E., Brann, M.R., 1991. Antagonist binding profiles of five cloned human muscarinic receptor subtypes. *J. Pharmacol. Exp. Ther.* 256, 727–733.
- Duisenberg, A.J.M., 1992. Indexing in single-crystal diffraction with an obstinate list of reflections. *J. Appl. Crystallogr.* 25, 92–96.
- Duisenberg, A.J.M., 1998. EvalCCD. PhD thesis, University of Utrecht, The Netherlands.
- Dwoskin, L.P., Crooks, P.A., 2001. Competitive neuronal nicotinic receptor antagonists: a new direction for drug discovery. *J. Pharmacol. Exp. Ther.* 298, 395–402.
- Eglen, R.M., Choppin, A., Watson, N., 2001. Therapeutic opportunities from muscarinic receptor research. *Trends Pharmacol. Sci.* 22, 409–414.
- Eiselé, J.-L., Bertrand, S., Galzi, J.-L., Devillers-Thiéry, A., Changeux, J.-P., Bertrand, D., 1993. Chimeric nicotinic-serotonergic receptor combines distinct ligand binding and channel specificities. *Nature* 366, 479–483.
- Enraf-Nonius, 1989. CAD-4 Software, Version 5.0. Enraf-Nonius, Delft, The Netherlands.
- Fitch, R.W., Xiao, Y., Kellar, K.J., Daly, J.W., 2003. Membrane potential fluorescence: a rapid and highly sensitive assay for nicotinic receptor channel function. *Proc. Natl. Acad. Sci. U. S. A.* 100, 4909–4914.
- Gotti, C., Fornasari, D., Clementi, F., 1997. Human neuronal nicotinic receptors. *Prog. Brain Res.* 53, 199–237.
- Hine, J., Cholod, M.S., King, R.A., 1974. Bifunctional catalysis of the deuteration of acetone-d₆ by 3-dimethylaminopropylamine, 2-(dimethylaminomethyl)cyclopentylamines, and polyethylenimines. *J. Am. Chem. Soc.* 96, 835–845.
- Holladay, M.W., Dart, M.J., Lynch, J.K., 1997. Neuronal nicotinic acetylcholine receptors as targets for drug discovery. *J. Med. Chem.* 40, 4169–4194.
- Jaroszewski, J.W., Matzen, L., Frølund, B., Krogsgaard-Larsen, P., 1996. Neuroactive polyamine wasp toxins: nuclear magnetic resonance spectroscopic analysis of the protolytic properties of philanthotoxin-343. *J. Med. Chem.* 39, 515–521.
- Jensen, A.A., Mikkelsen, I., Frølund, B., Bräuner-Osborne, H., Falch, E., Krogsgaard-Larsen, P., 2003. Carbamoylcholine homologs: novel and potent agonists at neuronal nicotinic acetylcholine receptors. *Mol. Pharmacol.* 64, 865–875.
- Johnson, C.K., 1976. ORTEP II Report ORNL-5138. A Fortran Thermal-Ellipsoid Plot Programme for Crystal Structure Illustrations. Oak-Ridge National Laboratory, Tennessee, USA.
- Karlin, A., 2002. Emerging structure of the nicotinic acetylcholine receptors. *Nat. Rev. Neurosci.* 3, 102–114.
- Kinas, R., Pankiewicz, K., Stec, W.J., Farmer, P.B., Foster, A.B., Jarman, M., 1977. Synthesis and absolute configuration of the optically active forms of 2-[bis(2-chloroethyl)amino]-4-methyltetrahydro-2H-1,3,2-oxazaphosphorine 2-oxide (4-methylcyclophosphamide). *J. Org. Chem.* 42, 1650–1652.
- Levin, E.D., 2002. Nicotinic receptors in the nervous system. In: Simon, S.A., Nicoletis, M.A.L. (Eds.), *Methods and New Frontiers in Neuroscience*. CRC Press, Boca Raton.
- Lindstrom, J., 1997. Nicotinic acetylcholine receptors in health and disease. *Mol. Neurobiol.* 152, 193–222.
- Nonius, 1999. COLLECT. Nonius, Delft, The Netherlands.
- Parker, M.J., Beck, A., Luetje, C.W., 1998. Neuronal nicotinic receptor $\beta 2$ and $\beta 4$ subunits confer large differences in agonist binding affinity. *Mol. Pharmacol.* 54, 1132–1139.
- Paterson, D., Nordberg, A., 2000. Neuronal nicotinic receptors in the human brain. *Prog. Neurobiol.* 61, 75–111.
- Perrin, C.L., Fabian, M.A., 1996. Multicomponent NMR titration for simultaneous measurement of relative pK_as. *Anal. Chem.* 68, 2127–2134.
- Punzi, J.S., Banerjee, S., Abood, L.G., 1991. Structure-activity relationships for various N-alkylcarbamyl esters of choline with selective nicotinic cholinergic properties. *Biochem. Pharmacol.* 41, 465–467.
- Ransom, R.W., Stec, N.L., 1988. Cooperative modulation of [³H]MK-801 binding to the N-methyl-D-aspartate receptor-ion channel complex by L-glutamate, glycine, and polyamines. *J. Neurochem.* 51, 830–836.
- Romanelli, M.N., Gualtieri, F., 2003. Cholinergic nicotinic receptors: competitive ligands, allosteric modulators, and their potential applications. *Med. Res. Rev.* 23, 393–426.
- Sabey, K., Paradiso, K., Zhang, J., Steinbach, J.H., 1999. Ligand binding and activation of rat nicotinic $\alpha 4\beta 2$ receptors stably expressed in HEK293 cells. *Mol. Pharmacol.* 55, 58–66.
- Sharples, C.G., Kaiser, S., Soliakov, L., Marks, M.J., Collins, A.C., Washburn, M., Wright, E., Spencer, J.A., Gallagher, T., Whiteaker, P., Wonnacott, S., 2000. UB-165: a novel nicotinic agonist with subtype selectivity implicates the $\alpha 4\beta 2^*$ subtype in the modulation of dopamine release from rat striatal synaptosomes. *J. Neurosci.* 20, 2783–2791.

- Sheldrick, G.M., 1986. SHELXS-86. Program for the Solution of Crystal Structures. University of Göttingen, Göttingen, Germany.
- Sheldrick, G.M., 1990. Phase annealing in SHELX-90: direct methods for larger structures. *Acta Crystallogr. A* 46, 467–473.
- Sheldrick, G.M., 1996. SADABS. Program for Absorption Correction. Bruker AXS Analytical X-ray Systems, Madison, Wisconsin, USA.
- Sheldrick, G.M., 1997. SHELXL97. Program for Crystal Structure Refinement. University of Göttingen, Göttingen, Germany.
- Sheldrick, G.M., 1997. SHELXS97. Program for the Solution of Crystal Structures. University of Göttingen, Göttingen, Germany.
- Silva, N.M., Tributino, J.L., Miranda, A.L., Barreiro, E.J., Fraga, C.A., 2002. New isoxazole derivatives designed as nicotinic acetylcholine receptor ligand candidates. *Eur. J. Med. Chem.* 37, 163–170.
- Søkkilde, B., Mikkelsen, I., Stensbøl, T.B., Andersen, B., Ebdrup, S., Krosgaard-Larsen, P., Falch, E., 1996. Analogues of carbacholine: synthesis and relationship between structure and affinity for muscarinic and nicotinic acetylcholine receptors. *Arch. Pharm. Pharm. Med. Chem.* 329, 95–104.
- Tulp, M., Bohlin, L., 2002. Functional versus chemical diversity: is biodiversity important for drug discovery? *Trends Pharmacol. Sci.* 23, 225–231.
- Wilson, A.J.C., 1995. *International Tables for Crystallography*, Vol. C; Tables 4.2.6.8 and 6.1.1.4. Kluwer Academic, Dordrecht, The Netherlands.
- Xiao, Y., Meyer, E.L., Thompson, J.M., Surin, A., Wroblewski, J., Kellar, K.J., 1998. Rat $\alpha 3/\beta 4$ subtype of neuronal nicotinic acetylcholine receptor stably expressed in a transfected cell line: pharmacology of ligand binding and function. *Mol. Pharmacol.* 54, 322–333.
- Zhong, W., Gallivan, J.P., Zhang, Y., Li, L., Lester, H.A., Dougherty, D.A., 1998. From ab initio quantum mechanics to molecular neurobiology: a cation- π binding site in the nicotinic receptor. *Proc. Natl. Acad. Sci. U. S. A.* 95, 12088–12093.